

## Accepted Manuscript

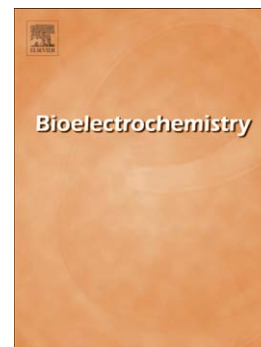
Triazole-linked phenyl derivatives: Redox mechanisms and *in situ* electrochemical evaluation of interaction with dsDNA

A. Dora R. Pontinha, Caterina M. Lombardo, Stephen Neidle, Ana Maria Oliveira-Brett

PII: S1567-5394(14)00126-1  
DOI: doi: [10.1016/j.bioelechem.2014.08.010](https://doi.org/10.1016/j.bioelechem.2014.08.010)  
Reference: BIOJEC 6780

To appear in: *Bioelectrochemistry*

Received date: 12 May 2014  
Revised date: 8 July 2014  
Accepted date: 13 August 2014



Please cite this article as: A. Dora R. Pontinha, Caterina M. Lombardo, Stephen Neidle, Ana Maria Oliveira-Brett, Triazole-linked phenyl derivatives: Redox mechanisms and *in situ* electrochemical evaluation of interaction with dsDNA, *Bioelectrochemistry* (2014), doi: [10.1016/j.bioelechem.2014.08.010](https://doi.org/10.1016/j.bioelechem.2014.08.010)

This is a PDF file of an unedited manuscript that has been accepted for publication. As a service to our customers we are providing this early version of the manuscript. The manuscript will undergo copyediting, typesetting, and review of the resulting proof before it is published in its final form. Please note that during the production process errors may be discovered which could affect the content, and all legal disclaimers that apply to the journal pertain.

## Triazole-linked phenyl derivatives: redox mechanisms and *in situ* electrochemical evaluation of interaction with dsDNA

A. Dora R. Pontinha<sup>1</sup>, Caterina M. Lombardo<sup>2</sup>, Stephen Neidle<sup>2</sup> and Ana Maria Oliveira-Brett<sup>1\*</sup>

<sup>1</sup> Department of Chemistry, University of Coimbra, 3004-535 Coimbra, Portugal

<sup>2</sup> UCL School of Pharmacy, University College London, London WC1N 1AX, UK

\*brett@ci.uc.pt

Ana Maria Oliveira-Brett  
Departamento de Química,  
Faculdade de Ciências e Tecnologia,  
Universidade de Coimbra,  
3004-535 Coimbra, Portugal  
Tel/FAX: +351-239-835295

### Abstract

The redox mechanism of two trisubstituted triazole-linked phenyl derivatives, (CL41 and CL42) and a disubstituted triazole-linked phenyl derivative (CL2r50), were studied using cyclic, differential pulse and square wave voltammetry at a glassy carbon electrode. The CL41, CL42 and CL2r50 oxidation is a complex, pH-dependent irreversible process involving the formation of electroactive products which undergo two consecutive reversible oxidation reactions. The DNA interaction with CL41, CL42 and CL2r50 was investigated by differential pulse voltammetry using the dsDNA-electrochemical biosensor and in DNA/trisubstituted triazole incubated solutions. All three trisubstituted triazole-linked phenyl derivatives interacted with dsDNA causing morphological and oxidative damage to the dsDNA structure in a time-dependent manner. The DNA-electrochemical biosensor enabled the detection of oxidative damage to DNA following the occurrence of the 8-oxoGua and/or 2,8-oxoAde oxidation peaks.

**Keywords:** substituted triazole-linked phenyl compounds, dsDNA electrochemical biosensor, voltammetry, glassy carbon electrode.

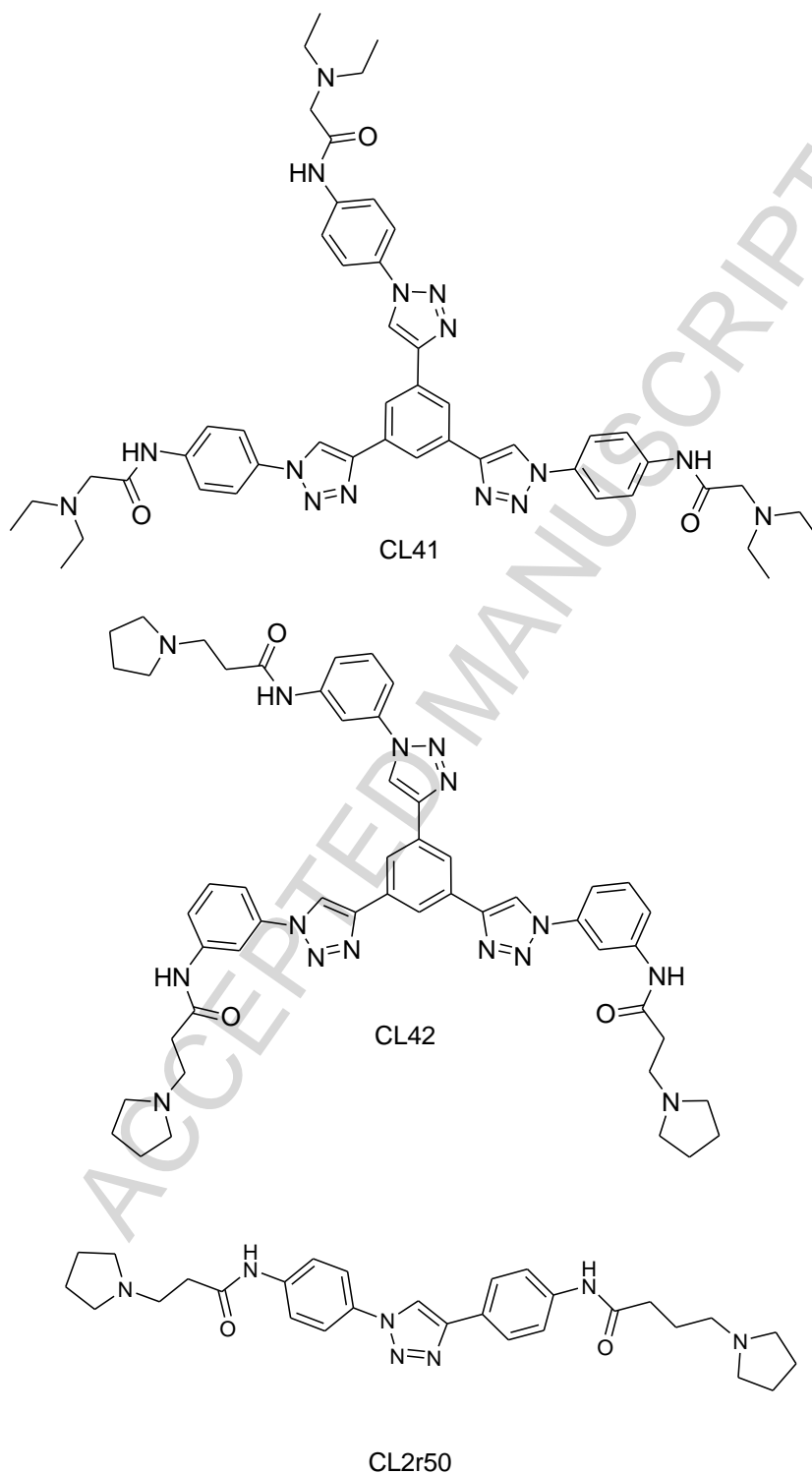
**Abbreviations:** dsDNA – double-stranded DNA

## 1. Introduction

Genomic DNA is a target for a large number of small therapeutic molecules [1, 2]. The overwhelming majority interact with double-helical DNA, which comprises almost all the genome, at least in eukaryotic organisms, and a number of such compounds, typified by the anthracycline drug doxorubicin, find clinical utility as anti-tumour agents in the treatment of human cancers [3]. The investigation of the intercalative interactions of such non-covalently binding compounds with duplex DNA has utilised a wide range of biophysical and biochemical approaches, so that the molecular details of drug binding have been extensively characterised. Intercalative compounds can also produce DNA damage in cells, with the role of the DNA damage response also being well-characterised [4].

Guanine (G)-rich DNA sequences are present in the telomeres of eukaryotic chromosomes and are prevalent in other regions of the genome, where they can form specialised four-stranded arrangements, termed G-quadruplexes [5, 6]. When stabilised by appropriate small molecules, these arrangements can inhibit the function of the specialised reverse transcriptase enzyme telomerase, whose expression is up-regulated in the majority of human cancers [7, 8]. A large number of such quadruplex-stabilising compounds have been identified, such as the 3,6,9-trisubstituted acridine compound BRACO-19 molecule [9, 10]. Although BRACO-19 binds to quadruplex DNA with high affinity, its affinity for duplex DNA is only some 30-fold lower. The design and synthesis of several mimetics of BRACO-19 with superior quadruplex selectivity was reported [11]. The ability of these compounds to induce both indirect DNA damage and oxidative damage to duplex and ultimately quadruplex DNA, is a potentially significant factor in their overall biological effect. The electrochemical redox behaviour of two members of a series of quadruplex-binding triazole–acridine conjugated compounds, GL15 and GL7 [12], and their *in situ* interaction with duplex DNA has been previously reported [13], together with the finding that their interaction with duplex DNA causes condensation of DNA morphology in a time-dependent manner. The use of a rapid method for the detection of DNA oxidative damage as applied to three quadruplex-binding compounds, two of which have been previously characterised as telomerase inhibitory is reported in this paper.

The acridine nucleus of the earlier compounds has been replaced in the triazole-phenyl conjugate compounds by a di- or tri-substituted phenyl ring with side-chains of appropriate length to contact quadruplex grooves [11]. These are compounds CL41, CL42 and CL2r50, **Scheme 1**. The two compounds with three alkylamino arms (CL41, CL42) are DNA groove-binders analogous to BRACO-19 [14,15]. These compounds were found experimentally to have greater affinity for the human telomeric quadruplex coupled with much lower affinity for duplex DNA compared to BRACO-19 [10].



**Scheme 1.** Chemical structures of CL42, CL41 and CL2r50.

Electrochemical research on DNA and small therapeutic molecules are of great relevance for explaining many biological mechanisms. The interpretation of the electrochemical data can contribute to the elucidation of the mechanisms by which DNA is oxidative damaged, as an approach to the behaviour in cells [16, 17].

The DNA-electrochemical biosensor is a sensitive and cost-effective model for simulating nucleic acid hazard compounds interaction. DNA is a highly charged, hydrophilic molecule, whereas the carbon electrode has a hydrophobic surface, and the spontaneous adsorption of DNA in a buffered solution on the carbon surface occurs [17].

Significant differences in the dsDNA and ssDNA peak currents were observed due to the rigidity of the double strand structure. The dsDNA structure hinders the electron transfer from the bases guanine and adenine inside the double helix. Whereas in ssDNA the bases are more exposed to the solution, which facilitates the interaction of the hydrophobic aromatic rings of the purines and pyrimidines with the hydrophobic carbon electrode substrate. Consequently, ssDNA interacts and adsorbs much more strongly to the carbon electrode surface, when compared with dsDNA, for the same solution concentration [18].

The DNA-electrochemical biosensor surface modifications were investigated for different DNA adsorption immobilization procedures, electrostatic adsorption or evaporation, leading to the formation of a monolayer or a multilayer DNA film. The immobilization of the DNA probe on the electrode surface is a very important factor for the optimal construction of a DNA-electrochemical biosensor [18-22].

Interactions of several compounds with duplex DNA have been previously studied using the DNA-electrochemical biosensor [18-22] and compared with other methods such as UV-Vis, IR and Raman spectroscopy, DNA footprinting, nuclear magnetic resonance mass spectroscopy, molecular modelling techniques, capillary electrophoresis, equilibrium dialysis, surface plasmon resonance, femtosecond laser spectroscopy and HPLC [23] showed greater sensitivity in the detection of small perturbations to the double-helical structure of DNA [24]. The detection of DNA oxidative damage has also enabled the unravelling of some of the detailed molecular interactions that occur. An important advantage of electrochemical detection of small molecule direct interaction with duplex DNA is that the drug-redox reaction may generate *in situ*, on the electrode surface, highly reactive intermediates that will immediately interact with duplex DNA.

The DNA structure can have more than one conformation in solution, depending on the pH and ionic environment. DNA double helices are classified either as A-DNA or B-DNA, the latter encompassing B-, C-, D-, E- and T-DNA, according to their conformations. Under physiological conditions, the dominant form is B-DNA. The rare A-DNA exists only in a dehydrated state, and although it has been shown that relatively dehydrated DNA fibers can adopt the A-conformation under physiological conditions, is still unclear whether DNA ever assumes this form *in vivo* [17].

Raman spectra studies revealed that a C-DNA form is produced at pH 4.0. The formation of C-DNA may be the result of an overall decrease in the charge of the polynucleotide chains; protonation permits closer approach of the phosphates [25-27]. In general, C-DNA resembles B-DNA, with conformation parameters of the nucleotide blocks changed only slightly [26].

The electrochemical characterization of substituted triazole-linked phenyl compounds CL41, CL42 and CL2r50, was investigated for a wide pH range between 2 and 12, using cyclic, square wave and differential pulse voltammetry at a glassy carbon electrode, together with the investigation of their interaction with duplex DNA in incubated solutions. A systematic study to elucidate the *in situ* interaction of CL41, CL42 and CL2r50 with dsDNA immobilized on a glassy carbon electrode surface using

a dsDNA-electrochemical biosensor was also undertaken. Similar experiments were also performed using single stranded homo-ribopolyribonucleotides of known sequences, and poly[G] and poly[A], to clarify the nature of the interaction between these compounds and the dsDNA.

## 2. Experimental

### 2.1 Materials and reagents

The tri-substituted triazole-phenyl conjugates, CL41, CL42 and CL2r50 were synthesized and purified [11].

Double-stranded DNA (dsDNA) (D1501), single stranded polyadenylic acid (poly[A]) (P9403) and polyguanylic acid (poly[G]) (P4404) were purchased from Sigma-Aldrich, and all were used without further purification.

The 0.1 M ionic strength electrolyte solutions [28] were: pH 2.0 KCl/HCl, pH 3.4-5.4 acetate buffer, pH 6.1-8.0 phosphate buffer, pH 9.2-10.5 ammonia buffer, and pH 12.0 NaOH/KCl were prepared using analytical grade reagents and purified water from a Millipore Milli-Q system (conductivity  $\leq 10 \mu\text{S}/\text{cm}$ ).

Stock solutions of 0.216 mM CL42, 0.336 mM CL41 and 0.272 mM CL2r50 were prepared in deionized water, added some drops of 0.2M HCl, and stored at 5 °C. Solutions of different concentrations were obtained by dilution of the appropriate volume in the supporting electrolyte.

All stock solutions were in weight, 300  $\mu\text{g}/\text{mL}$  dsDNA, poly[G] and poly[A], prepared in deionized water and diluted to the desired concentrations in pH = 4.5 (0.1 M acetate buffer).

Nitrogen saturated solutions were obtained by bubbling high purity  $\text{N}_2$  for a minimum of 10 min in the solution and continuing with a flow of pure gas over the solution during the voltammetric experiments. All experiments were done at room temperature,  $T = 298 \text{ K}$  (25 °C).

Microvolumes were measured using EP-10 and EP-100 Plus Motorized Microliter Pipettes (Rainin Instrument Co. Inc., Woburn, USA). The pH measurements were carried out with a Crison micropH 2001 pH-meter with an Ingold combined glass electrode.

### 2.2 Voltammetric parameters and electrochemical cells

Voltammetric experiments were carried out using a  $\mu\text{Autolab}$  potentiostat with GPES 4.9 software (Eco-Chemie, Utrecht, The Netherlands). The measurements were carried out in a solution volume of 0.5 mL, using a three-electrode system one-compartment electrochemical cell of capacity 2 mL (Bio-Logic SAS, France). A glassy carbon electrode (GCE,  $d = 1.5 \text{ mm}$ ) was the working electrode, a Pt wire the counter electrode and an Ag/AgCl (3M KCl) reference electrode (Bio-Logic SAS, France). The experimental conditions were: for cyclic voltammetry (CV) scan rate 100 mV/s, and for differential pulse (DP) voltammetry pulse amplitude 50 mV, pulse width 70 ms and scan rate 5 mV/s. Square wave voltammetry conditions were frequency 25 Hz and potential increment 2 mV, corresponding to an effective scan rate 100 mV/s.

The glassy carbon electrode (GCE) was polished using a diamond spray (particle size 3  $\mu\text{m}$ ) (Kemet, UK) before each electrochemical experiment. After polishing, it was rinsed thoroughly with Milli-Q water. Following this mechanical treatment, the GCE was placed in buffer supporting electrolyte and differential pulse voltammograms were

recorded until a steady state baseline voltammogram was obtained. This procedure ensured very reproducible experimental results.

### 2.3 Acquisition and presentation of voltammetric data

Differential pulse voltammograms presented were background-subtracted and baseline-corrected using the moving average application with a step window of 5 mV included in the GPES v 4.9 software. This mathematical treatment improves the visualization and identification of peaks over the baseline without introducing any artefact, although the peak intensity is, in some cases, reduced (<10%) relative to that of the untreated curve. Nevertheless, this mathematical treatment of the original voltammograms was used in the presentation of all experimental voltammograms for an improved and clearer identification of the peaks. The values for peak current presented in all plots were determined from the original untreated voltammograms after subtraction of the baseline.

### 2.4 DNA-biosensor preparation and incubation procedure

The multi-layer dsDNA-electrochemical biosensor was prepared by electrostatic immobilization, covering the GCE ( $d = 1.5$  mm) surface with three successive drops of 5  $\mu$ L each of 50  $\mu$ g/mL dsDNA solution, and this repeated procedure ensured completely coverage of the GCE surface by dsDNA. The DNA concentration was in weight and the results using a multi-layer dsDNA-electrochemical biosensor on the GCE surface are all qualitative.

After placing each drop on the electrode surface the biosensor was dried under a constant flux of  $N_2$  and afterwards was applied a potential of + 0.30 V vs Ag/AgCl during 5 min, where no electron transfer reaction of the DNA components occurs, leading to a much stronger DNA immobilization, and enhancing the robustness and stability of the dsDNA nano-films on the GCE surface [29].

Incubations were always carried out immersing the DNA-electrochemical biosensors in [CL41] = 50  $\mu$ M, [CL42] = 50  $\mu$ M or [CL2r50] = 5  $\mu$ M, and pH = 4.5 (0.1M acetate buffer), solutions under continuously stirring, during different periods of time. The modified electrode was always gently washed with deionized water before transferring to acetate buffer to assure the removal of unbounded trisubstituted triazole-linked phenyl compound.

Incubation with 300  $\mu$ g/mL dsDNA was carried out by keeping the GCE during different periods of time in solutions containing [CL41] = 50  $\mu$ M, [CL42] = 50  $\mu$ M or [CL2r50] = 5  $\mu$ M in pH 4.5 (0.1 M acetate buffer) at room temperature.

## 3. Results and discussion

The electrochemical behaviour of three triazole-linked phenyl derivatives, CL41, CL42 and CL2r50, for a wide supporting electrolyte pH range at GCE was first studied. The phenyl-triazole derivatives interaction with dsDNA *in situ* using the DNA-electrochemical biosensor and incubated solutions was also investigated.

### 3.1 Redox behaviour of the triazole-linked phenyl derivatives CL41, CL42 and CL2r50

#### 3.1.1 Cyclic voltammetry

The electrochemical behaviour of the phenyl-triazole derivatives, CL41, CL42

and CL2r50, was investigated using a GCE by CV in pH = 5.4 (0.1 M acetate buffer). The CVs showed peaks only in the positive region, **Figs. 1-3**, and no peaks were observed in the negative region. During the potential scanning a constant flow of N<sub>2</sub> over the solution, to prevent diffusion of atmospheric oxygen into the solution, was maintained.

The redox current is proportional to the electron transfer rate. Different concentrations of the phenyl-triazole derivatives were used according to the redox currents and different electron transfer rates obtained of each compound, **Figs. 1-3**. The oxidation of the CL41, CL42 and CL2r50, showed irreversible oxidation peaks and .

**Here Fig. 1**

The first CV scan in [CL41] = 150 μM showed two irreversible peaks, peak 1<sub>a</sub>, at  $E_{p1a} = + 0.84$  V, and peak 2<sub>a</sub>, at  $E_{p2a} = + 1.18$  V, **Fig. 1**. In the second CV scan two new anodic peaks, peak 3<sub>a</sub>, at  $E_{p3a} = + 0.35$  V, and peak 4<sub>a</sub>, at  $E_{p4a} = + 0.63$  V, and the correspondent cathodic peaks, peak 3<sub>c</sub>, at  $E_{p3c} = + 0.19$  V, and peak 4<sub>c</sub>, at  $E_{p4c} = + 0.35$  V, appeared. These peaks correspond to the quasi-reversible redox reactions of CL41 oxidation products. Successive CVs showed a big decrease of the oxidation peak 1<sub>a</sub> and 2<sub>a</sub> currents due to the adsorption of CL41 and/or its non-electroactive oxidation products on the GCE surface.

The redox behaviour of CL42 and CL2r50 was also studied by CV under the same conditions. The first CV in [CL42] = 75 μM showed two anodic peaks, peak 1<sub>a</sub>, at  $E_{p1a} = + 0.98$  V, and peak 2<sub>a</sub>, at  $E_{p2a} = + 1.06$  V, **Fig. 2**, no reduction peak was observed, and the oxidation of CL42 was irreversible.

**Here Fig. 2**

The CVs in [CL2r50] = 150 μM showed that the CL2r50 oxidation occurs in three irreversible steps, with the formation of two electroactive products that undergo quasi-reversible oxidations, **Fig. 3**.

**Here Fig. 3**

### 3.1.2 Differential pulse voltammetry and effect of pH

DP voltammetry of phenyl-triazole derivatives, CL41, CL42 and CL2r50, was studied in a pH range between 3.4 and 12.0 aqueous buffer supporting electrolytes, **Fig. 4**.

**Here Fig. 4**

DP voltammograms in [CL41] = 50 μM, in pH = 5.4 (0.1 M acetate buffer), showed two oxidation peaks, peak 1<sub>a</sub> and peak 2<sub>a</sub>, **Fig. 4A**. Successive DP voltammograms in the same solution without cleaning the GCE surface showed two new peak, peak 3<sub>a</sub> and peak 4<sub>a</sub>, corresponding to the oxidation of the CL41 oxidation product, **Fig. 4A**. For pH < 9.0, both peak potentials were shifted to more negative values with increasing pH, **Fig 4B**. The dependence followed the relationship  $E_{p1a}$  (V) = 1.08 – 0.059 pH for peak 1<sub>a</sub>, and  $E_{p2a}$  (V) = 1.38 – 0.059 pH for peak 2<sub>a</sub>, **Fig. 4B**,

indicating that the oxidation mechanism in both peaks occurs with the transfer of the same number of electrons and protons [30]. As for peak 1<sub>a</sub>,  $W_{1/2} \sim 110$  mV, and for peak 2<sub>a</sub>,  $W_{1/2} \sim 87$  mV, it can be concluded that the mechanism of oxidation of CL41 occurs in two steps with one electron-one proton transfer [30]. For pH > 9.0 the oxidation of CL41 is pH-independent indicating a mechanism involving only the transfer of one electron and the value of  $pK_a \approx 9$  for CL41 was determined.

DP voltammograms obtained in [CL42] = 50  $\mu$ M, in pH = 5.4 (0.1 M acetate buffer), also showed two oxidation peaks, peak 1<sub>a</sub>, at  $E_{p1a} = + 0.85$  V, and peak 2<sub>a</sub>, at  $E_{p2a} = + 0.96$  V, **Fig. 4C**. In a second DP scan, in the same solution without cleaning the GCE surface, two new peaks occurred, peak 3<sub>a</sub> and peak 4<sub>a</sub>. These peaks correspond to the oxidation of CL42 oxidation product. At the same time, the oxidation peaks 1<sub>a</sub> and 2<sub>a</sub> decreased gradually with the number of scans due to the decrease of the available electrode surface because of adsorption of CL42 and/or CL42 oxidation products on the GCE surface. The oxidation peak 1<sub>a</sub> only appears for  $2 < \text{pH} < 6$ , and the potential decreased with increasing pH, **Fig. 4D**. The peak 2<sub>a</sub> occurs in all supporting electrolytes and the potential was shifted to more negative values with increasing pH, **Fig. 4D**. The dependence of 59 mV per pH unit, and width at half-height, for peak 1<sub>a</sub>,  $W_{1/2} \sim 100$  mV, and for peak 2<sub>a</sub>,  $W_{1/2} \sim 90$  mV, showed that each CL42 oxidation process involved one electron-one proton transfer, **Fig. 4D**.

DP voltammograms in [CL2r50] = 10  $\mu$ M in pH = 5.4 (0.1 M acetate buffer), showed three oxidation peaks, **Fig 4E**. The oxidation of CL2r50 is pH dependent and the variation of  $E_{pa}$  versus pH is linear, following the relationships: for peak 1<sub>a</sub>,  $E_{p1a}$  (V) =  $- 0.072 - 0.060$  pH,  $W_{1/2} \sim 87$  mV, corresponding to an oxidation mechanism with one electron-one proton transfer; for peak 2<sub>a</sub>,  $E_{p2a}$  (V) =  $- 0.32 - 0.060$  pH,  $W_{1/2} \sim 60$  mV, and for peak 3<sub>a</sub>,  $E_{p3a}$  (V) =  $- 0.32 - 0.060$  pH,  $W_{1/2} \sim 60$  mV, each corresponding to two electron-two proton transfer, **Fig.4F**. In the second DP voltammogram, in the same solution without cleaning the GCE surface, two new peaks, peak 4<sub>a</sub> and peak 5<sub>a</sub>, corresponding to the oxidation of CL2r50 oxidation products, **Fig.4E**, occurred.

The CL2r50 oxidation products peak potentials were shifted to more negative values with increasing pH, following the relationships: for peak 4<sub>a</sub>,  $E_{p4a}$  (V) =  $0.54 - 0.059$  pH, and for peak 5<sub>a</sub>,  $E_{p5a}$  (V) =  $0.75 - 0.059$ , **Fig. 5**. The slope of 59 mV per pH unit and  $W_{1/2} \approx 90$  mV for both peaks corresponding to oxidation mechanisms with one electron-one proton transfer.

**Here Fig. 5**

The oxidation currents for the electron transfer reaction of CL42, CL41 and CL2r50 at pH = 4.5 were always greater than at the other pHs investigated.

### 3.1.3 Square wave voltammetry

Square wave (SW) voltammetry experiments were carried out for the three triazole-linked phenyl derivatives for the same pH range. Since the current is sampled in both positive and negative-going pulses, peaks corresponding to the oxidation and reduction of the electroactive species at the electrode surface can be obtained in the same experiment. The reversibility of the first peak was confirmed by plotting the

forward ( $I_f$ ) and backward ( $I_b$ ) current component where the oxidation and reduction currents are equal.

SW voltammogram in [CL41] = 50  $\mu$ M in pH = 5.4 (0.1 M acetate buffer) showed two irreversible peak 1<sub>a</sub>, at  $E_{p1a}$  = + 0.87 V, and peak 2<sub>a</sub>, at  $E_{p2a}$  = + 1.20 V, **Fig. 6A**, and the irreversibility of the first peak was confirmed. In the second SW voltammogram recorded without clearing the CGE, two new peaks occurred, peak 3<sub>a</sub>, at  $E_{p3a}$  = + 0.36 V, and peak 4<sub>a</sub>, at  $E_{p4a}$  = + 0.53 V, corresponding to the reversible oxidation of CL41 products, **Fig. 6B**.

**Here Fig. 6**

The first SW voltammogram in [CL42] = 50  $\mu$ M in pH = 7.0 (0.1 M phosphate buffer) showed the irreversibility of peak 2<sub>a</sub>,  $E_{p2a}$  = + 0.71 V, **Fig. 6C**. The oxidation peak 1<sub>a</sub> only appears for 2 < pH < 6. In the second scan two anodic peaks, corresponding reversible oxidation of CL42 oxidation products, peak 3<sub>a</sub>, at  $E_{p3a}$  = + 0.13 V, and peak 4<sub>a</sub>, at  $E_{p4a}$  = + 0.42 V, **Fig. 6D**, occurred.

The SW voltammograms in [CL2r50] = 50  $\mu$ M in pH = 4.3 (0.1 M acetate buffer) showed in the first scan three irreversible oxidation peaks, peak 1<sub>a</sub>, at  $E_{p1a}$  = + 0.91 V, peak 2<sub>a</sub>, at  $E_{p2a}$  = + 1.07 V, and peak 3<sub>a</sub>, at  $E_{p3a}$  = + 1.18 V, **Fig. 6E**, and in the second scan two reversible, peak 4<sub>a</sub> and 5<sub>a</sub>, in a similar behaviour to the other phenyl-triazole derivatives, **Fig. 6F**.

### 3.2 Triazole-acridine conjugates-dsDNA interaction

Following the study of CL41, CL42 and CL2r50 oxidation mechanisms the interaction with dsDNA of CL41, CL42 and CL2r50, using dsDNA-, poly [G], and poly[A]-electrochemical biosensors and dsDNA-phenyl-triazole derivatives in incubated solutions was investigated.

The knowledge of the oxidation potentials of the purine dsDNA bases dGuo, at  $E_{pa}$  = + 0.98 V, dAdo, at  $E_{pa}$  = + 1.24 V [20-22] enabled the correct identification of the DNA-triazole-acridine conjugates interaction.

#### 3.2.1. Triazole-acridine conjugates-dsDNA in incubated solutions

DP voltammograms were obtained after incubation periods of 0, 6 and 24 h in pH = 4.5 (0.1M acetate buffer) of 300  $\mu$ g/mL dsDNA with [CL42] = 50  $\mu$ M, [CL41] = 50  $\mu$ M or [CL2r50] = 5  $\mu$ M.

Control solutions of 300  $\mu$ g /mL dsDNA were also prepared and analysed after the same periods of time and the control DP voltammogram of the dsDNA solution showed two peaks corresponding to the oxidation of desoxyguanosine (dGuo), at  $E_{pa}$  = + 0.98 V, and desoxyadenosine (dAdo), at  $E_{pa}$  = + 1.24 V, **Fig. 7**.

**Here Fig. 7**

DP voltammograms recorded immediately after addition of CL41 to the dsDNA solution, showed four peaks due to the oxidation of the purine dsDNA bases dGuo, at  $E_{pa}$  = + 0.98 V, dAdo, at  $E_{pa}$  = + 1.24 V and CL41 oxidation peaks 1<sub>a</sub> and 2<sub>a</sub>, at  $E_{p1a}$  = + 0.87 and at  $E_{p2a}$  = + 1.15 V, **Fig. 7**. Increasing the incubation time, the guanine and adenine oxidation peak currents decreased compared with the control dsDNA solution, showing that dsDNA condensed after the DNA-CL41 interaction.

DP voltammograms obtained after 6 h incubation showed an increase in all peak currents but they were lower compared with the dsDNA control peaks, **Fig. 7**. This is due to the structural changes, strand breaks and intercalation of CL41 in dsDNA, causing the purine bases to be more in contact with the electrode surface and available for electrochemical oxidation. The peak at  $E_{pa} = + 0.80$  V corresponds to the oxidation of CL41 intercalated in the dsDNA and/or the oxidation of free guanine released from dsDNA, which occur at the same potential.

Similar results were also obtained for CL42 and CL2r50, **Fig. 8**. DP voltammograms showed CL42 and CL2r50 oxidation peaks followed by the dsDNA oxidation peaks and the occurrence of the same two new peaks: at  $E_{pa} = + 0.45$  V and at  $E_{pa} = + 0.80$  V.

**Here Fig. 8**

The intercalation of the CL41, CL42 and CL2r50 quadruplex binders in the DNA structure [12, 31] was detected by the occurrence of the 8-oxoGua and/or 2,8-oxoAde oxidation peak, at  $E_{pa} = + 0.45$  V.

The experiments were also performed using solutions of 100  $\mu\text{g/mL}$  single stranded poly[G] and poly[A] homopolyribonucleotides to obtain more information concerning the preferential interaction of the purine bases, guanine or adenine, with the dsDNA.

DP voltammograms recorded after different incubation periods showed a decrease in the dAdo and dGuo oxidation peak currents with increasing incubation time when compared with the control solutions. The results demonstrated that, in  $\text{pH} = 4.5$ , the compounds CL42, CL41 and CL2r50 caused no oxidative damage to poly[G] and poly[A] homopolyribonucleotides, since no 8-oxoGua and/or 2,8-oxoAde oxidation peak was observed. These results are explained by the greater stability of poly[G] and poly[A] homopolyribonucleotides secondary structures formed in  $\text{pH} = 4.5$ , making the phenyl triazole derivatives interaction more difficult.

### **3.2.2. Triazole-acridine conjugates-dsDNA interaction using dsDNA-electrochemical biosensors**

The interaction between the dsDNA and CL41, CL42 and CL2r50, was also investigated using dsDNA-electrochemical biosensors. The dsDNA-electrochemical biosensor consists of an electrode with DNA immobilized on the surface. The interaction of the compound with surface immobilized dsDNA causes changes of the DNA structure which can be followed by the changes in the oxidation peaks of dsDNA purinic bases dGuo, at  $E_{pa} = + 0.91$  V, dAdo, at  $E_{pa} = + 1.17$  V [20-22].

Complete coverage of the electrode surface was necessary [29] to avoid undesired non-specific binding and was obtained using the multilayer dsDNA-electrochemical biosensor, prepared as described in *Section 2.4*. The interaction of dsDNA with the compounds triazole-acridine conjugates, CL41, CL42 and CL2r50, was followed with time by DP voltammetry.

The dsDNA-electrochemical biosensor prepared was incubated, for different periods of time, 5, 10 and 20 min, in  $[\text{CL42}] = 10 \mu\text{M}$  and afterwards transferred to  $\text{pH} = 7.0$  (0.1 M phosphate buffer) where DP voltammograms were recorded, **Fig. 9**.

**Here Fig. 9**

For low incubation times,  $t = 5$  min, the decrease of DNA oxidation peaks, due to the aggregation/condensation of DNA immobilized on the electrode surface, because the purines electroactive centres are hidden inside the rigid structure being unable to reach the GCE surface, and consequently unavailable for electrochemical oxidation, was observed. A progressive decrease of dsDNA bases oxidation peak currents was observed with increasing incubation time. The decrease of dGuo and dAdo oxidation peak currents corresponded to the dsDNA condensation. The results obtained were similar to those in incubated solutions. However, a new oxidation peak due to 8-oxoGua and/or 2,8 oxoAde oxidation, at  $E_{pa} = + 0.34$  V, and the oxidation peak due to the oxidation of free guanines released from dsDNA, at  $E_{pa} = + 0.67$  V, were observed.

The same results were also observed for the interaction of CL2r50 and CL41 with the dsDNA-electrochemical biosensor, demonstrating that, in  $pH = 4.5$ , the compounds CL42, CL41 and CL2r50 caused oxidative damage to dsDNA.

#### 4. Conclusions

The electrochemical behaviour of the three phenyl-triazole derivatives (CL41, CL42 and CL2r50), was carried out over a wide pH range, and is an irreversible, pH-dependent electron transfer process, involving the formation of electrochemically detected reversible electroactive products.

The interaction between dsDNA-phenyl-triazole derivatives was investigated in incubated solutions and using dsDNA-electrochemical biosensors showing that the all three phenyl-triazole compounds induced structural changes and strand breaks in the dsDNA structure in a time-dependent manner, and oxidative damage to dsDNA was electrochemically also detected by the occurrence of 8-oxoGua and/or 2,8-oxoAde oxidation peak.

The dsDNA-electrochemical biosensors enabled a qualitative fast determination of the affinity and selectivity of molecules binding to DNA and the detection of the oxidative damage to dsDNA by these phenyl-triazole derivatives, and detecting the perturbations caused to the dsDNA morphologic structure by an external cause may contribute to clarify the *in vivo* mechanisms.

#### Acknowledgements

Financial support from Fundação para a Ciência e Tecnologia (FCT), PhD grant SFRH/BD/46026/2008 (A.D.R. Pontinha), projects PTDC/QEQ-MED/0586/2012, PEst-C/EME /UI0285/2013 and CENTRO-07-0224-FEDER-002001 (MT4MOBI) (co-financed by the European Community Fund FEDER), FEDER funds through the program COMPETE – Programa Operacional Factores de Competitividade, is gratefully acknowledged. Work in the S.N. laboratory was supported by Programme Grant No. C129/A4489, from Cancer Research UK, and by a Cancer Research UK research studentship to CML.

## References

- [1] S. Neidle. DNA minor groove recognition by small molecules. *Natural Prod. Reports* 18 (2001) 291-309.
- [2] L.H. Hurley. DNA and its associated processes as targets for cancer therapy. *Nat Rev Cancer* 2 (2002) 188-200
- [3] G. Tacar, P. Sriamornsak, C. R. Dass. Doxorubicin: an update on anticancer molecular action, toxicity and novel drug delivery systems. *J Pharm Pharmacol.* 65 (2013) 157-170.
- [4] R.A. Forrest, L.P. Swift, A. Rephaeli, A. Nudelman, K. Kimura, D.R. Phillips, S.M. Cutts. Activation of DNA damage response pathways as a consequence of anthracycline-DNA adduct formation. *Biochem Pharmacol.* 83 (2012) 1602-1612.
- [5] M.L. Bochman, K. Paeschke, V.A. Zakian. DNA secondary structures: stability and function of G-quadruplex structures. *Nature Rev Genet.* 13 (2012) 770-780.
- [6] E.Y. Lam, D. Beraldi, D. Tannahill, S. Balasubramanian. G-quadruplex structures are stable and detectable in human genomic DNA. *Nat Commun.* 4 (2013) 1796.
- [7] A. De Cian, L. Lacroix, C. Douarre, N. Temime-Smaali, C. Trentesaux, J.-F. Riou, J.-L. Mergny, Targeting telomeres and telomerase, *Biochimie* 90 (2008) 131-155.
- [8] M. Franceschin, G-quadruplex DNA Structure and Organic Chemistry: More Than One Connection, *Eur. J. Org. Chem.* 14 (2009) 2225-2238.
- [9] M. Read, R.J. Harrison, R. Romagnoli, F.A. Tanious, S.H. Gowan, A.P. Reszka, W.D. Wilson, L.R. Kelland, S. Neidle, Structure-based design of selective and potent G quadruplex-mediated telomerase inhibitors. *Proc. Natl. Acad. Sci. U.S.A.* 98 (2001) 4844-4849.
- [10] M. Gunaratnam, O. Greciano, C. Martins, A.P. Reszka, C.M. Schultes, H. Morjani, J.-F. Riou, S. Neidle, Mechanism of acridine-based telomerase inhibition and telomere shortening, *Biochem. Pharmacol.* 7 (2007) 679-689.
- [11] C.M. Lombardo, I.S. Martínez, S. Haider, V. Gabelica, E. De Pauw, J.E. Moses, S. Neidle, Structure-based design of selective high-affinity telomeric quadruplex-binding ligands, *Chem. Commun.* 46 (2010) 9116-9118.
- [12] S. Sparapani, S.M. Haider, F. Doria, M. Gunaratnam, S. Neidle, Rational design of acridine-based ligands with selectivity for human telomeric quadruplexes, *J. Am. Chem. Soc.* 132 (2010) 12263-12272.
- [13] A.D.R. Pontinha, S. Sparapani, S. Neidle, A.M. Oliveira-Brett, Triazole-acridine conjugates: Redox mechanisms and in situ electrochemical evaluation of interaction with double-stranded DNA, *Bioelectrochemistry* 89 (2013) 50-56.
- [14] N. H. Campbell, G. N. Parkinson, A. P. Reszka and S. Neidle. Structural basis of DNA quadruplex recognition by an acridine drug. *J. Amer. Chem. Soc.* 130 (2008) 6722-6724.
- [15] S. Neidle, Telomeric Quadruplex Ligands I: Anthraquinones and Acridines, in: *Therapeutic Applications of Quadruplex Nucleic Acids*. Elsevier/Academic Press, Amsterdam, 2012, pp. 67-91 Chapter 4.
- [16] G.M. Blackburn, M.J. Gait, *Nucleic Acids in Chemistry and Biology*, Oxford University Press, UK, 1996.
- [17] W. Saenger, *Principles of Nucleic Acid Structure*, Springer-Verlag, New York, 1984.

- [18] A.M. Oliveira-Brett, S.H.P. Serrano, J.A.P. Piedade, *Electrochemistry of DNA in: R.G. Compton, E.G. Hancock (Eds.), Comprehensive Chemical Kinetics, vol. 37, Elsevier, Amsterdam, 1999, pp. 91-119 Chapter 3.*
- [19] A.M. Oliveira Brett, S.H.P. Serrano, T.A. Macedo, D. Raimundo, M.H. Marques, M.A. La-Scalea, *Electrochemical determination of carboplatin in serum using a DNA-modified glassy carbon electrode, Electroanalysis 7 (1996) 992-995.*
- [20] S.C.B. Oliveira, A.M. Chiorcea-Paquim, S.M. Ribeiro, A.T.P. Melo, M. Vivan, A.M. Oliveira-Brett, *In situ electrochemical na AFM study of thalidomide-DNA interaction, Bioelectrochemistry 76 (2009) 201-207.*
- [21] A.-M. Chiorcea-Paquim, O. Corduneanu, S.C.B. Oliveira, V.C. Diculescu, A.M. Oliveira-Brett, *Electrochemical and AFM evaluation of hazard compounds-DNA interaction, Electrochim. Acta 54 (2009) 1978-1985.*
- [22] A.D.R. Pontinha, S.M. Jorge, A.M. Chiorcea-Paquim, V.C Diculescu, A.M. Oliveira-Brett, *In situ evaluation of anticancer drug methotrexate-DNA interaction using a DNA-electrochemical biosensor and AFM characterization, Phys Chem Chem Phys. 13 (2011) 5227-5234.*
- [23] S. Rauf, J.J. Gooding, K. Akhtar, M.A. Ghauri, M. Rahman, M.A. Anwar, A.M. Khalid, *Electrochemical approach of anticancer drugs-DNA interaction, J. Pharmaceut. Biomedic. 37 (2005) 205-217.*
- [24] C.M.A. Brett, A.M. Oliveira-Brett, in *Encyclopedia of Electrochemistry, (A. J. B. a. M. Stratmann, Ed.s), Wiley-VCH Verlag, Weinheim, Vol. 3, Germany, 2003, 105-124.*
- [25] T. O'Connor, S. Mansy, M. Bina, D.R. McMillin, M.A. Bruck, R.S. Tobias, *The pH-dependent structure of calf thymus DNA studied by Raman spectroscopy., Biophys. Chem. 15 (1982) 53-64.*
- [26] S.B. Zimmerman, B.H. Pfeiffer, *Does DNA adopt the C form in concentrated salt solutions or in organic solvent/water mixtures? An X-ray diffraction study of DNA fibers immersed in various media. J. Mol. Biol. 142 (1980) 315-330.*
- [27] R. Langridge, D.A. Marvin, W.E. Seeds, H.R. Wilson, C.W. Hooper, M.H.F. Wilkins, L.D. Hamilton, *The molecular configuration of deoxyribonucleic acid: II. Molecular models and their fourier transforms. J. Mol. Biol. 2 (1960) 38-62.*
- [28] D.D. Perrin, B. Dempsey, *Buffers for pH and Metal Ion Control, J. Wiley, 1974.*
- [29] S.C.B. Oliveira, A.M. Oliveira-Brett, *DNA-Electrochemical biosensors: AFM surface characterisation an application to detection of in situ oxidative damage to DNA, Comb. Chem. High T. Scr. 13 (2010) 628-640.*
- [30] C.M.A. Brett, A.M. Oliveira Brett, *Electrochemistry: Principles, Methods and Applications, Oxford Science University Publications ed., Oxford, U.K., 1993.*
- [31] B.C. Baguley, L.P.G. Wakelin, J.D. Jacintho, P. Kovacic, *Mechanisms of action of DNA intercalating acridine-based drugs: How important are contributions from electron transfer and oxidative stress?, Curr. Med. Chem. 10 (2003) 2643-2649.*

## Figures

**Fig. 1** CVs obtained in 150  $\mu\text{M}$  CL41 solution in pH = 5.4 phosphate buffer,  $\text{N}_2$  saturated, (—) first, (•••) second and (---) sixth scans,  $v = 100 \text{ mV/s}$ .

**Fig. 2** CVs obtained in 75  $\mu\text{M}$  CL41 solution in pH = 5.4 phosphate buffer,  $\text{N}_2$  saturated, (—) first, (•••) second and (---) sixth scans,  $v = 100 \text{ mV/s}$ .

**Fig. 3** CVs obtained in 150  $\mu\text{M}$  CL2r50 solution pH = 5.4 phosphate buffer,  $\text{N}_2$  saturated, (—) first, (•••) second and (---) sixth scans,  $v = 100 \text{ mV/s}$ .

**Fig. 4** (A, C and E) DP voltammograms base line corrected in pH 5.4 (0.1 M acetate buffer), (—) first and (•••) second scans, scan rate 5 mV/s; (B, D and F) Plots of  $E_{\text{pa}}$  vs. pH. (A, B) [CL41] = 50  $\mu\text{M}$ ; (C, D) [CL42] = 50  $\mu\text{M}$  and (E, F) [CL2r50] = 10  $\mu\text{M}$ ; peak 1<sub>a</sub> (■), peak 2<sub>a</sub> (○) and peak 3<sub>a</sub> (▲).

**Fig. 5** Plot in [CL2r50] = 10 $\mu\text{M}$  of (■)  $E_{\text{p4a}}$  and (○)  $E_{\text{p5a}}$  vs. pH.

**Fig. 6** SW voltammograms in 50  $\mu\text{M}$  solutions, first and second scans: (A, B) CL41 in pH = 5.4 (0.1 M acetate buffer); (C, D) CL42 in pH = 7.0 (0.1 M phosphate buffer); (E, F) CL2r50 in pH = 4.3 (0.1M acetate buffer),  $I_t$  –total current,  $I_f$  – forward and  $I_b$  – backward current components,  $v_{\text{ef}} = 100 \text{ mV/s}$ .

**Fig. 7** DP voltammograms base line corrected in pH = 4.5 (0.1 M acetate buffer): (—) 300  $\mu\text{g/mL}$  dsDNA control, (—) [CL41] = 50  $\mu\text{M}$  control, and after incubation with dsDNA during: 0h (•••), 6h (---) and 24h (•••).

**Fig. 8** DP voltammograms base line corrected in pH = 4.5 (0.1 M acetate buffer): (—) 300  $\mu\text{g/mL}$  dsDNA control, (A) (—) [CL42] = 50  $\mu\text{M}$  control and (B) (—) [CL2r50] = 5  $\mu\text{M}$  control, and after incubation with dsDNA during: 0h (•••), 6h (---) and 24h (•••).

**Fig. 9** DP voltammograms base line corrected in pH = 7.0 (0.1 M phosphate buffer): (—) dsDNA-electrochemical biosensors control and (—) [CL42] = 10  $\mu\text{M}$  control, and after dsDNA-electrochemical biosensors incubation with [CL42] = 10  $\mu\text{M}$  during: (---) 5, (•••) 10 and (•••) 20 min.

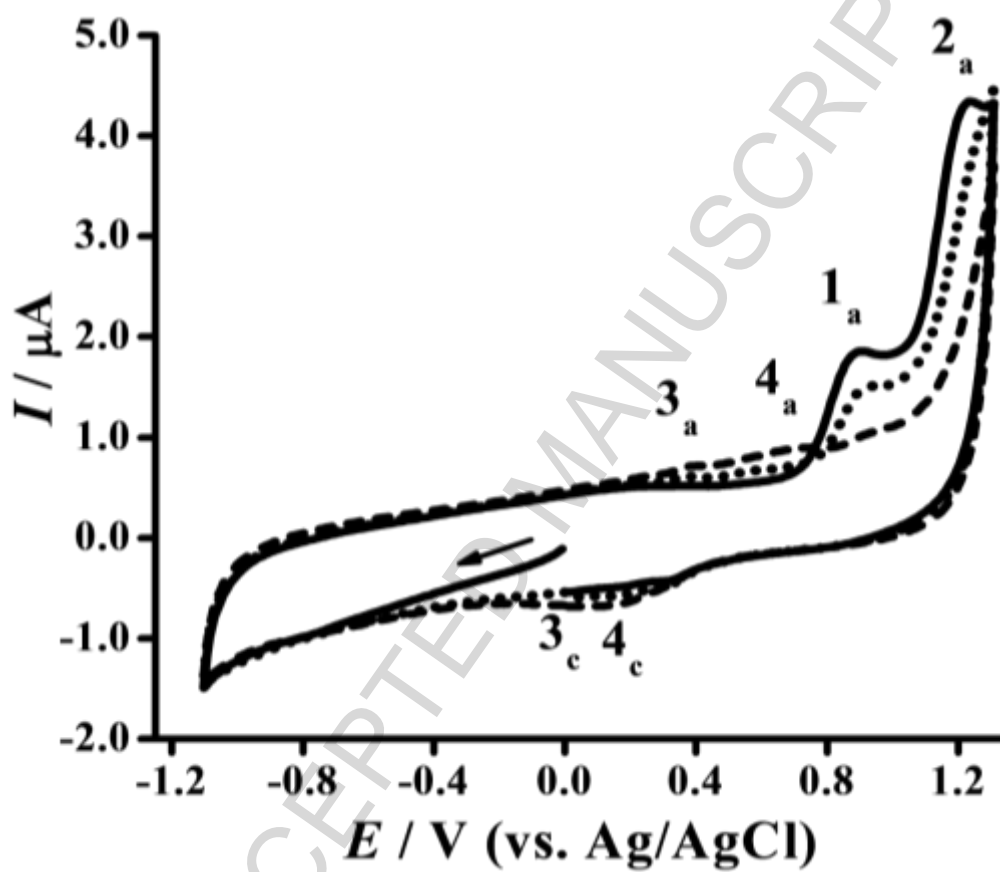


Fig. 1

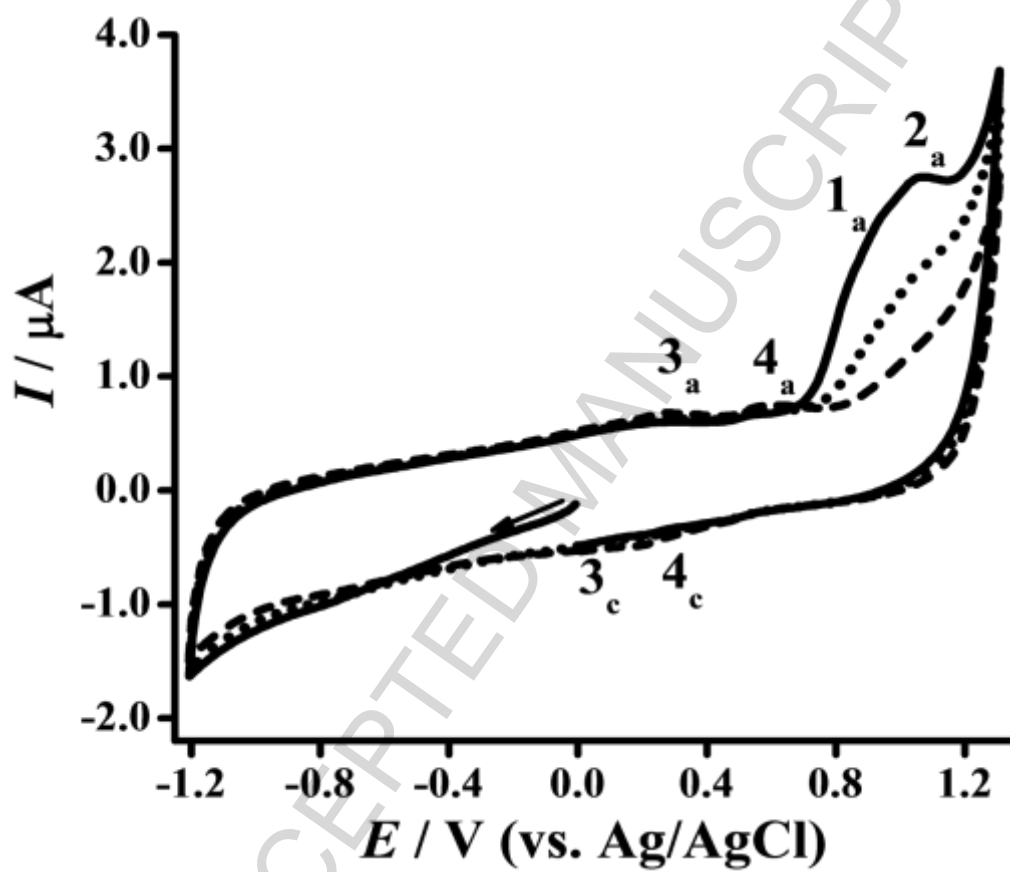


Fig. 2

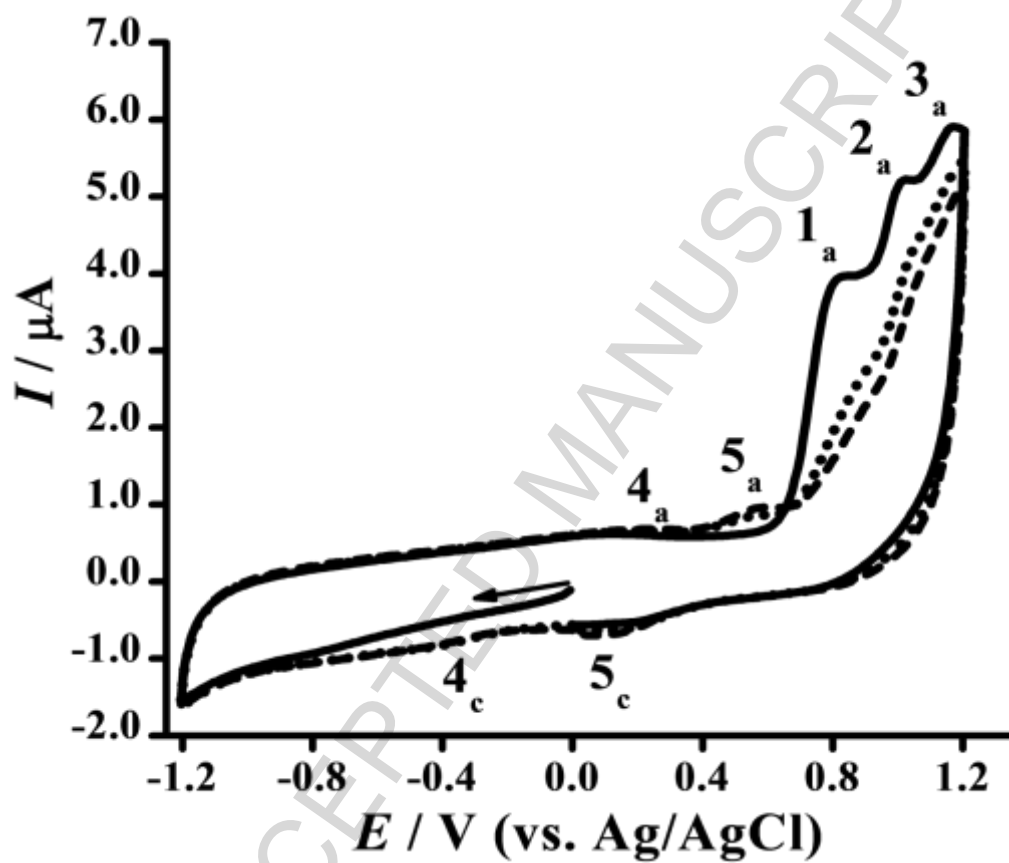


Fig. 3

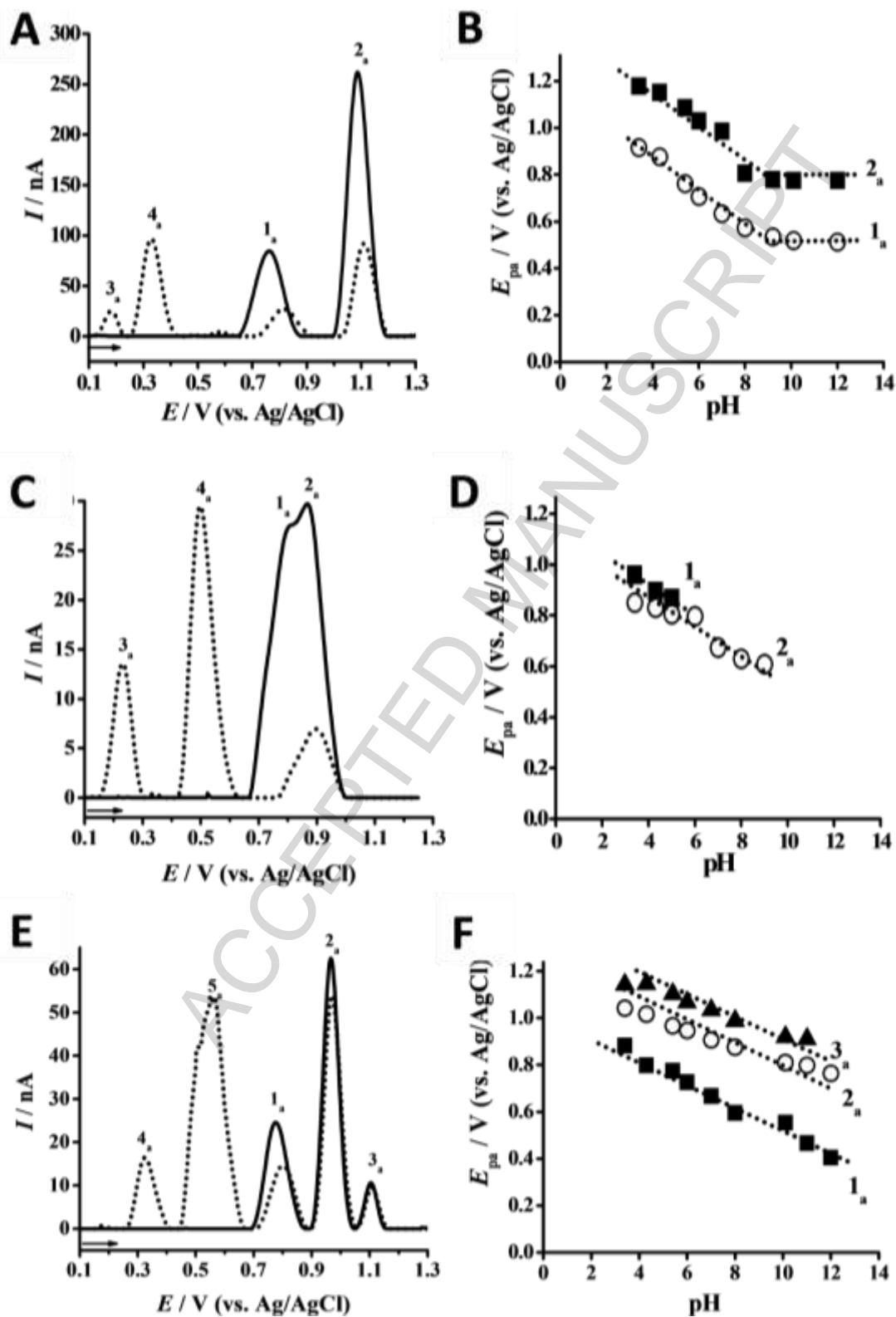


Fig. 4

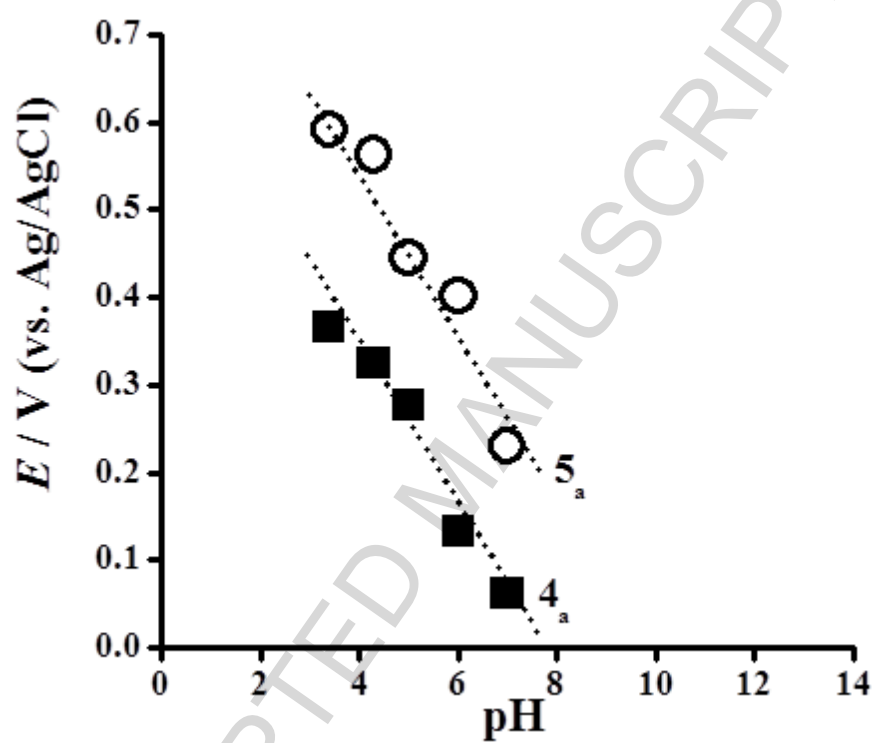


Fig. 5

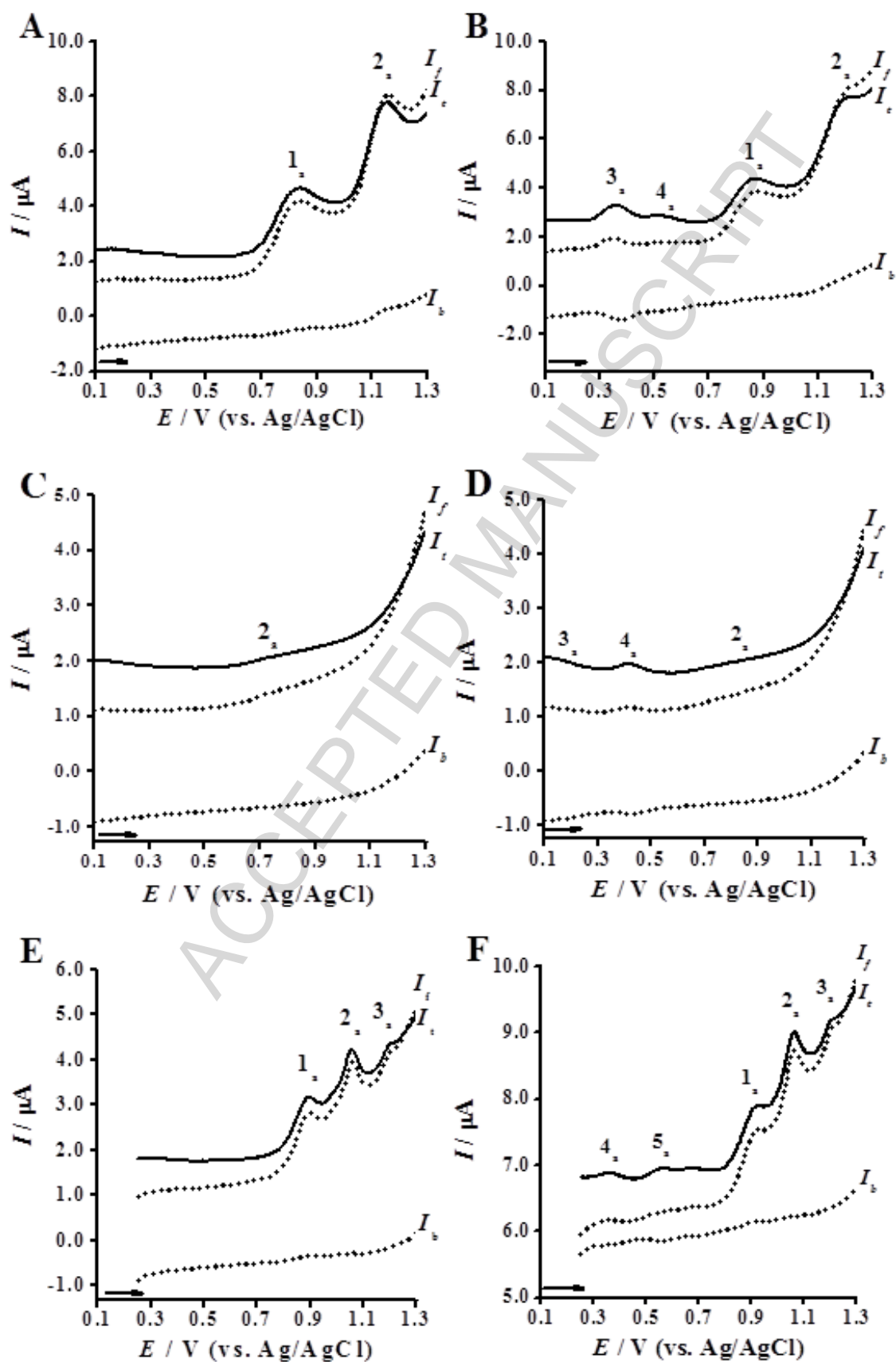


Fig. 6

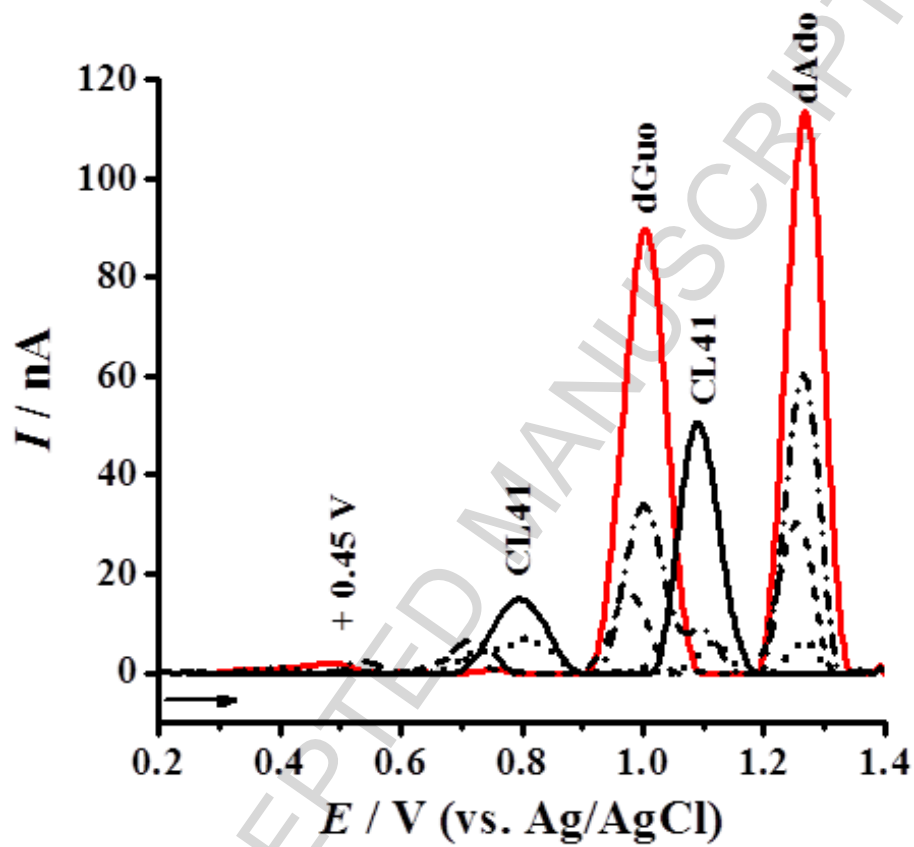


Fig. 7

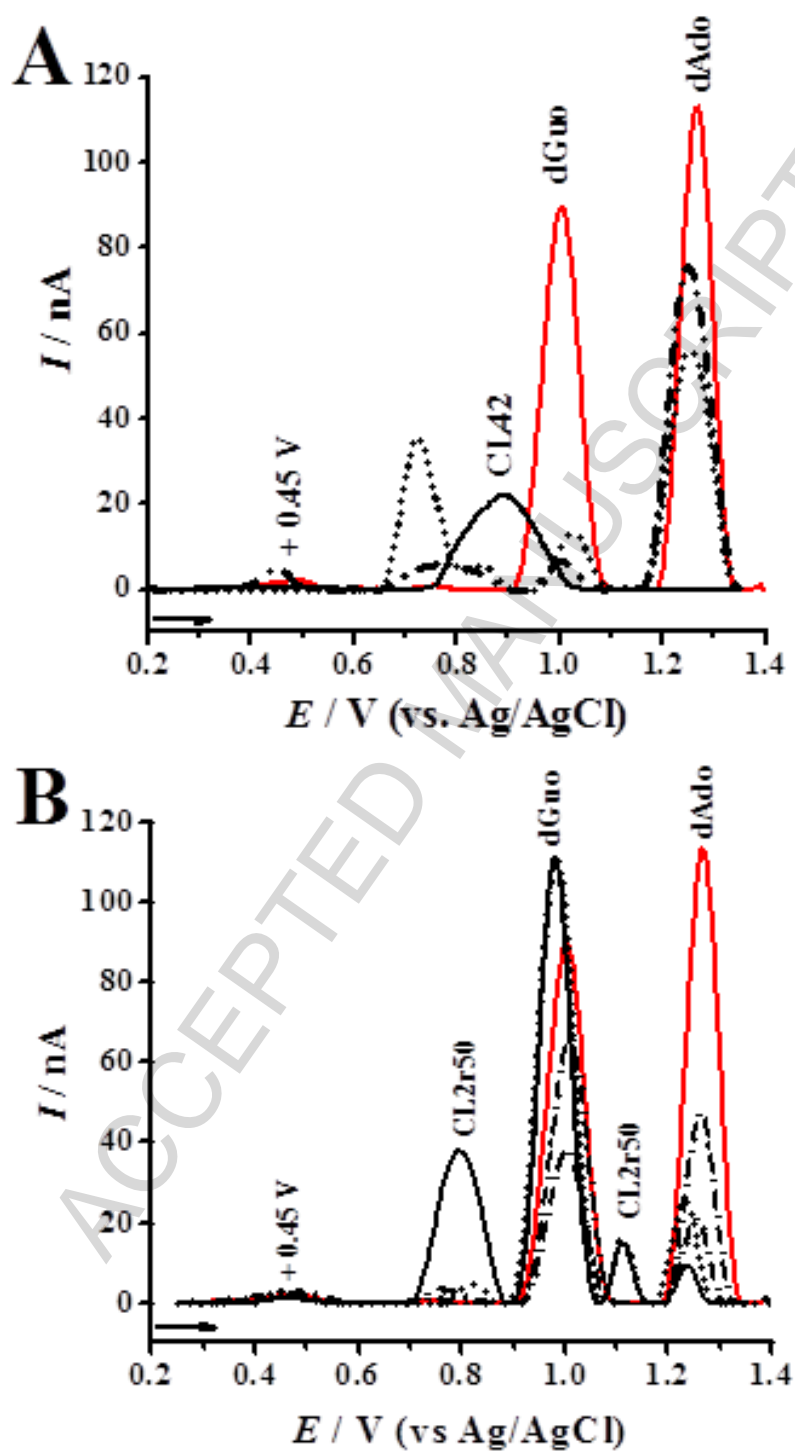


Fig. 8

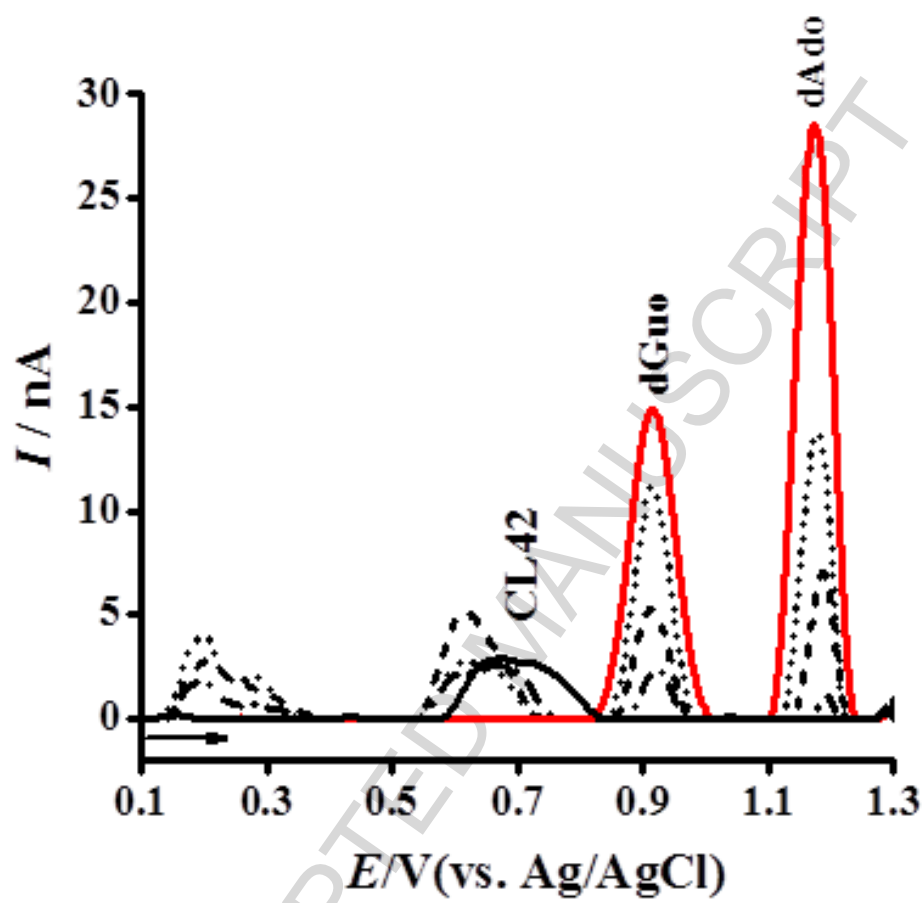


Fig. 9

## Triazole-linked phenyl derivatives: redox mechanisms and *in situ* electrochemical evaluation of interaction with dsDNA

A. Dora R. Pontinha<sup>1</sup>, Caterina M. Lombardo<sup>2</sup>, Stephen Neidle<sup>2</sup> and  
Ana Maria Oliveira-Brett<sup>1\*</sup>

<sup>1</sup> Department of Chemistry, University of Coimbra, 3004-535 Coimbra, Portugal

<sup>2</sup> UCL School of Pharmacy, University College London, London WC1N 1AX,  
UK

### Highlights

- Investigation of the pH-dependent redox mechanism of triazole-linked phenyl derivatives telomerase inhibitors for a wide pH range
- *In situ* evaluation of DNA-triazole-linked phenyl derivatives in incubated solutions and using a DNA-electrochemical biosensor
- The detection of oxidative damage to the dsDNA structure using differential pulse voltammetry
- The three phenyl-triazole derivatives induced structural changes in dsDNA and oxidative damage to the dsDNA structure in a time-dependent manner